RSC Advances

ROYAL SOCIETY
OF CHEMISTRY

www.rsc.org/advances

Luminescent Properties of Ag(I)/Cu(I) Coordination Polymers: Crystal Structures and Highly Intensity Luminescence of PMMA-Doped Hybrid Material Based on Quinoline-2,3-Dicarboxylic Acid Ligand

Yang Song[a], Rui-Qing Fan[a*], Hui-Jie Zhang[a], Zhi-Wei Liu[a], Xue-Tao Wang[a], Cai-Tu Tan[a], Yu-Lin Yang[a*] and Yu-Lei Wang[b]

[a] Department of Chemistry, Harbin Institute of Technology, Harbin 150001, P. R. of China

[b]National Key Laboratory of Science and Technology on Tunable Laser, Harbin Institute of Technology, Harbin 150080, P. R. of China

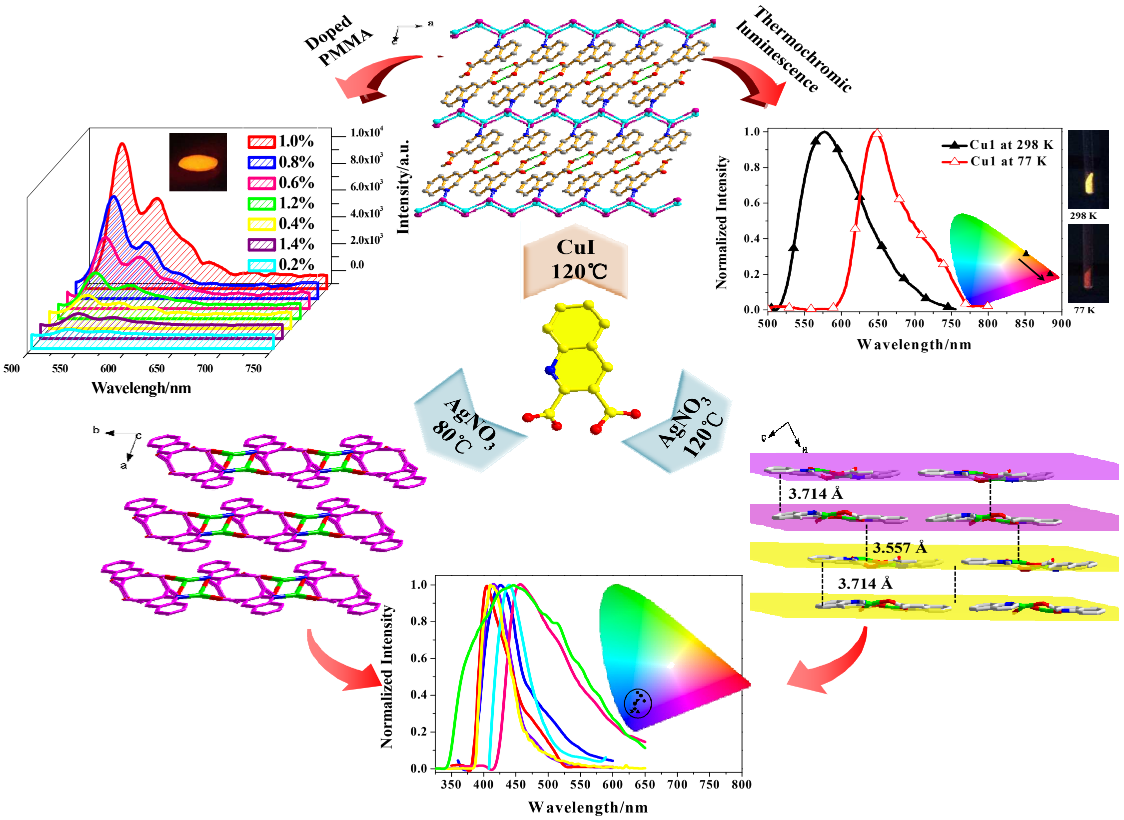

Preparation, characterization, crystal structure and different luminescent properties of Ag(I)/Cu(I) coordination polymers: stable blue emission, thermochromism and PMMA-doped hybrid material.

Luminescent Properties of Ag(I)/Cu(I) Coordination Polymers: Crystal Structures and Highly Intensity Luminescence of PMMA-Doped Hybrid Material Based on Quinoline-2,3-Dicarboxylic Acid Ligand

Yang Song[a], Rui-Qing Fan[a*], Hui-Jie Zhang[a], Zhi-Wei Liu[a], Xue-Tao Wang[a], Cai-Tu Tan[a], Yu-Lin Yang[a*] and Yu-Lei Wang[b]

[a] Department of Chemistry, Harbin Institute of Technology, Harbin 150001, P. R. of China

[b]National Key Laboratory of Science and Technology on Tunable Laser, Harbin Institute of Technology, Harbin 150080, P. R. of China

To whom the correspondence should be sent:

Prof. Rui-Qing Fan
Department of Chemistry
Harbin Institute of Technology Harbin 150001, P. R. China
Fax: +86-0451-86413710
E-mail: fanruiqing@hit.edu.cn and ylyang@hit.edu.cn

Abstract

Three one-dimensional (1D) Ag(I)/Cu(I) coordination polymers, formulated as $[Ag(2,3\text{-}Hqldc)]_n$(**Ag1**) , $[Ag(3\text{-}qlc)]_{2n}$(**Ag2**) and $[CuI(3\text{-}Hqlc)]_n$(**Cu1**) based on ligand quinoline-2,3-dicarboxylic acid (H_2qldc), were synthesized through hydrothermal(solvothermal) method and structurally characterized by single-crystal X-ray diffraction, IR spectroscopy and elemental analysis. Molecular structural analysis reveals that **Ag1** was a 1D + 1D → 1D infinite chain synthesized at a relatively low temperature 80 °C, which further forms three-dimensional (3D) structure by π–π stacking interaction. **Ag2** forms 1D dimer chain structure and via $\pi\cdots\pi$ packing interactions show two-dimensional (2D) supramolecular network. Both **Ag1** and **Ag2** display stable blue luminescent in the solid state and in organic solvents(DMSO, CH_3CN and CH_3OH) at 298 K and 77 K. However, **Cu1** posseses 1D ladder chain structure, which further forms 2D structure by hydrogen bonding interaction. **Cu1** shows tunable luminescence at 298 K and 77 K in the solid state with the large red-shift of 70 nm and the CIE color shifts from bright yellow (0.51, 0.48) to red (0.67, 0.30), indicating thermochromic luminescence for **Cu1**. After doping poly(methylmethacrylate) (PMMA), not only the luminescence intensity and lifetimes are enhanced but also the thermal stability is increased in comparison with **Cu1**. After **Cu1** doped with PMMA(**Cu1**@PMMA), the lifetime of polymer film materials **Cu1**@PMMA increases and reaches a maximum at 1.0% (τ = 95.57 μs), which is more than eight times longer than that of **Cu1** (τ = 13.78 μs). **Cu1**@PMMA is confirmed as a bright yellow luminescence polymer film material.

Introduction

Silver(I) and copper(I) coordination polymers have interesting luminescent properties[1] that have been utilized in areas such as light emitting diodes, luminescence probes[2] and emitting layers in polymer light-emitting diodes[3]. Although the coordination polymers have better luminescence and higher thermal stability, polymer-doped systems have clear technical advantages over glass ones, such as flexibility and prominent processing ability, which is important for optical fibers and fiber amplifiers[4]. When Isamu Akasaki, Hiroshi Amano and Shuji Nakamura produced bright blue light beams from their semi-conductors in the early 1990s, they triggered a fundamental transformation of lighting technology. Red and green diodes had been around for a long time but without blue light, white lamps could not be created. Despite considerable efforts, both in the scientific community and in industry, the blue LED had remained a challenge for three decades[5]. As luminescent materials, silver(I) coordination polymers can be used as stable blue luminescent complexes[6] in optical devices. However, until now, only a few cases have been reported about blue emitting silver(I) coordination polymers, and the realization of highly luminescence efficiency remains a big challenge[7].

In addition, monovalent copper complexes show a variety of structure and rich photophysical properties. Nevertheless, Cu(I) is easy to oxidize into Cu(II) in the process of synthesis, thus create monovalence copper complexes as luminescent material is difficult but very meaningful. A popular polymer matrix used as a host for luminescent transition coordination polymers is poly- (methyl methacrylate) (PMMA), which is a low-cost, simply prepared polymer with excellent optical quality[8]. Until now most of the reports are rare earth doped with PMMA[9]. There is no doubt that rare earth element shows excellent luminescent properties, but luminous color of rare earth element has defects which is not easy to control. Compared with noble metal Pt, Au, Ag even rare earth, Cu(I) with the advantage of cheap and non-poison, which also can modify ligands and control the emitting. Hence, copper-based systems with favorable luminescence are beginning to receive more attention[10]. When copper(I) coordination polymers incorporate with PMMA forming a new complex-containing polymer/film[11], it will lead to significant flexibility, versatility, thermal and photostability[12].

In this work, we choose quinoline-2,3-dicarboxylic acid (H_2qldc) as the ligand. H_2qldc as a derivative of 2,3-H_2pydc which has a relatively large π-conjugated system in the quinoline ring, which might not only contribute to the desirable fluorescence properties resulting from the interaction between 2,3-qldc^{2-} anions and metal ions, but also easily assemble into high dimensionality, supramolecular networks via π··π packing interactions between two adjacent aromatic rings as well as hydrogen bonding interactions. To the best of knowledge, cases of metal-organic complexes linked by H_2qldc have been presented. Y. P. Cai[13], J. H. Lin[14], G. B. Che[15] and their co-workers use 2,3-H_2qldc ligand to prepare a series of coordination polymers from zero- to two-dimension with Co(II), Zn(II), Cd(II), Mn(II) and Ln(III) ions, which are summarized in Table S1.

Three Ag(I)/Cu(I) coordination polymers constructed from H_2qldc, namely, $[Ag(2,3\text{-Hqldc})]_n$ (**Ag1**), $[Ag(3\text{-qlc})]_{2n}$(**Ag2**) and $[CuI(3\text{-Hqlc})]_n$(**Cu1**) have been synthesized under hydrothermal conditions. During the solvothermal synthetic process, unexpected situ decarboxylation of H_2qldc was observed. Through controlling the temperature (from 80 °C to 120 °C) makes the ligand 2,3-H_2qldc decarboxylation and results in the formation of 3-Hqlc ligand. After decarboxylation, the dihedral angle between the planes of carboxyl and quinoline in one bridging organic ligand is 3.70° in the **Ag2**, which is much smaller than those of 61.98° and 30.49° in the **Ag1**. The nice coplanar feature of the structure in **Ag2** can enhance the luminescent efficiency. The structure of **Ag2** has been reported by C. B. Liu, et al[16], but they directly use 3-Hqlc as ligand rather than decarboxylation of H_2qldc. In this work, we mainly talked about the decarboxylation process of H_2qldc and compared with coordination polymer **Ag1**. What's more, we also discussed the luminescent properties of **Ag1** and **Ag2** in details. Both **Ag1** and **Ag2** display stable blue luminescent in the solid state and in different solvents (DMSO, CH_3CN and CH_3OH) at 298 K and 77 K. However, **Cu1** shows the interesting property of thermochromic luminescence, which is rarely reported in literatures, and most of cases only talked about the luminescent properties in the solid state rather than the effect of solvent and temperature, more comparisons are summarized in Table S2.

Experimental section

General Characterization

All reagents were analytical grade (99.7%) from commercial sources and were used directly without any further purification. Elemental analyses (C, H, and N) were performed on a Perkin-Elmer 240c elemental analyzer. IR spectra were recorded by Nicolet Impact 410 FTIR spectrometer (range in 4000–400 cm^{-1}). ^{13}C NMR and ^{1}H NMR spectra were recorded on a Bruker ACF 400 MHz at room temperature. X–ray powder diffraction (XRPD) patterns were analyzed with monochromated Cu Kα radiation of 40 mA, 40 kV. UV-vis spectra were recorded on a Perkin-Elmer Lambda 20 spectrometer. The solid-state and solution photoluminescence analyses were carried out on an Edinburgh FLS920 fluorescence spectrometer in the range of 200–800 nm at 298 K and 77 K.

Synthesis of $[Ag(2,3\text{-}Hqldc)]_n$(Ag1)

A mixture of $AgNO_3$ (0.034 g, 0.20 mmol), 2,3-H_2qldc (0.021 g, 0.10 mmol) with a mole ratio of 2:1 was dissolved in 8 mL H_2O and stirred for 20 min. The final mixture was placed in a Teflon-lined stainless steel vessel (20 mL) under autogenous pressure and heated at 80 °C for 5 days. After slowly cooling to the room temperature, the mixture was washed with distilled water and colorless block-shaped crystals were filtered off and dried at room temperature (yield ca. 65%, based on silver metal). Elemental analysis (%): Calc. for $C_{11}H_6AgNO_4$ (Mr: 324.04): C, 40.77 ; N, 4.32 ; H, 1.87 %. Found: C, 40.72 ; N, 4.38 ; H, 1.89 %. IR (cm^{-1}): 3515 (br, s), 3404 (br, s), 3142 (w), 2235 (m), 1591 (vs), 1372 (vs), 1285 (s), 1132 (vs), 1001 (m), 750 (vs), 673 (s), 553 (w), 476 (w). ^{1}H NMR (400 MHz, DMSO–d_6): δ = 8.98 (s, 1 H, H_2qldc–H_1), 8.24 (s, 1 H, H_2qldc–H_5), 8.14 (d, 1 H, H_2qldc–$H_{4'}$), 7.95 (d, 1 H, H_2qldc–H_2), 7.77 (d, 1 H, H_2qldc–H_3) ppm. ^{1}H NMR (400 MHz, CD_3CN): δ = 9.13 (s, 1 H, H_2qldc–H_1), 8.24 (s, 1 H, H_2qldc–H_5), 8.18 (d, 1 H, H_2qldc–H_4), 8.06 (d, 1 H, H_2qldc–H_2), 7.84 (d, 1 H, H_2qldc H_3) ppm. ^{1}H NMR (400 MHz, CD_3OD): δ = 8.94 (s, 1 H, H_2qldc–H_1), 8.13 (d, 2 H, H_2qldc–$H_{4,5}$), 7.95 (d, 1 H, H_2qldc–H_2), 7.76 (d, 1 H, H_2qldc- H_3) ppm.

Synthesis of $[Ag(3\text{-qlc})]_{2n}$(Ag2)

A mixture of $AgNO_3$ (0.034 g, 0.20 mmol), 2,3-H_2qldc (0.021 g, 0.10 mmol), with a mole ratio of 2:1 was dissolved in 8 mL H_2O and stirred for 20 min. The final mixture was placed in a Teflon-lined stainless steel vessel (20 mL) under autogenous pressure and heated at 120 °C for 5 days. After slowly cooling to the room temperature, the mixture was washed with distilled water and colorless block-shaped crystals were filtered off and dried at room temperature (yield ca. 52%, based on silver metal). Elemental analysis (%): Calc. for $C_{20}H_{12}Ag_2N_2O_4$ (Mr: 560.06): C, 42.89; N, 5.00; H, 2.16 %. Found: C, 42.85; N, 5.03; H, 2.19 %. IR (cm^{-1}): 3437 (br, s), 3044 (w), 1597 (vs), 1558 (vs), 1394 (vs), 1317 (s), 793 (vs), 761 (m), 586 (m), 476 (w). ^1H NMR (400 MHz, DMSO–d_6): δ = 9.32 (s, 1 H, 3-qlc–H_1), 9.01 (s, 1 H, 3-qlc–H_2), 8.20 (d, 1 H, 3-qlc–H_6), 8.12 (d, 1 H, 3-qlc-H_3), 7.89 (d, 1 H, 3-qlc–H_5), 7.67 (d, 1 H, 3-qlc–H_4) ppm. ^1H NMR (400 MHz, CD_3CN): δ = 9.39 (s, 1 H, 3-qlc–H_1), 9.84 (s, 1 H, 3-qlc–H_2), 8.13 (d, 2 H, 3-qlc–$H_{3,5}$), 7.89 (d, 1 H, 3-qlc-H_6), 7.71 (d, 1 H, 3-qlc–H_4) ppm. ^1H NMR (400 MHz, CD_3OD): δ = 9.39 (s, 1 H, 3-qlc–H_1), 9.05 (s, 1 H, 3-qlc–H_2), 8.28 (s, 1 H, 3-qlc–H_6), 8.13 (d, 1 H, 3-qlc-H_3), 7.93 (d, 1 H, 3-qlc–H_5), 7.74 (d, 1 H, 3-qlc–H_4) ppm.

Synthesis of $[CuI(3\text{-Hqlc})]_n$(Cu1)

A mixture of CuI (0.019 g, 0.10 mmol), 2,3-H_2qldc (0.011 g, 0.05 mmol) with a mole ratio of 2:1 was dissolved in 6 mL CH_3CN and stirred for 20 min. The final mixture was placed in a Teflon-lined stainless steel vessel (20 mL) under autogenous pressure and heated at 120 °C for 5 days. After cooling to the room temperature, the mixture was washed with distilled water and yellow block-shaped crystals were filtered off and dried at room temperature (yield ca. 72%, based on copper metal). Elemental analysis (%): Calc. for $C_{10}H_7CuINO_2$ (Mr: 363.61): C, 33.00; N, 3.85; H, 1.93 %. Found: C, 33.59; N, 3.88; H, 1.96 %. IR (cm^{-1}): 3437 (br, s), 3076 (br, m), 1700 (vs), 1613 (vs), 1427 (m), 1285 (vs), 925 (w), 782 (vs), 465 (w). ^1H NMR (400 MHz, DMSO–d_6): δ = 9.40 (s, 1 H, 3-qlc–H_1), 9.16 (s, 1 H, 3-qlc–H_2), 8.32 (d, 2 H, 3-qlc–$H_{3,5}$), 7.93 (d, 1 H, 3-qlc–H_6), 7.78 (d, 1 H, 3-qlc–H_4) ppm. ^1H NMR (400 MHz, CD_3CN): δ = 9.40 (s, 1 H, 3-qlc–H_1), 8.89 (s, 1 H, 3-qlc–H_2), 8.13 (d, 2 H, 3-qlc–$H_{3,5}$), 7.89 (s, 1 H, 3-qlc-H_6), 7.67 (s, 1 H, 3-qlc–H_4) ppm. ^1H NMR (400 MHz, CD_3OD): δ = 9.93 (s, 1 H, 3-qlc–H_1), 9.59 (s, 1 H, 3-qlc–H_2), 8.86 (d, 1 H, 3-qlc–H_6), 8.70 (d, 1 H, 3-qlc-H_3), 8.51 (d, 1 H, 3-qlc–H_5), 8.28 (d, 1 H, 3-qlc–H_4) ppm.

Synthesis of Cu^+ Complex-Doped PMMA Polymer Films

The PMMA polymer was doped with the Cu(I) coordination polymer **Cu1** in the proportions 0.2, 0.4, 0.6, 0.8, 1.0, 1.2 and 1.4% (w/w). The PMMA powder was dissolved in 6 mL *N,N′*–dimethylformamide (DMF), followed by addition of the required amount of coordination polymer **Cu1** in DMF solution, and the resulting mixture was heated at 40 °C for 60 min. The polymer film was obtained after evaporation of excess solvent at 60 °C.

Syntheses

Hydrothermal methods are widely used in the syntheses of inorganic–organic polymers, especially when organic carboxylate ligands are applied. Because under such reaction conditions, the problems of ligand solubility can be minimized[17]. The structures of **Ag1** and **Ag2** were accomplished by introducing the N and O containing ligands into the reaction system, which may act as deprotonation and decarboxylation reagents. Coordination polymers **Ag1** and **Ag2** reported here were synthesized under hydrothermal reaction conditions, while reaction temperature showed a remarkable influence on the final structure. **Ag1** was synthesized at a relatively low temperature 80 °C to get the 1D + 1D → 1D infinite chain, which is forms by the H_2qldc with μ_2–η^1: η^1: η^0: η^0 bridging mode and **Ag1** further forms three-dimensional (3D) structure by π–π stacking interaction. **Ag2** was synthesized at a higher temperature 120 °C, forming 1D dimer chain structure and via π···π packing interactions show two-dimensional (2D) supramolecular network. Meanwhile, after replacing $AgNO_3$ with CuI, and changing water to organic solvent CH_3CN, **Cu1** was synthesized at a higher temperature 120 °C, which formed a 1D ladder chain.

Interestingly, the decarboxylation of H_2qldc was observed in the solvothermal synthetic process of **Ag2** and **Cu1**. In order to study the decarboxylation process of H_2qldc, a series of control experiments were conducted. We did the experiment under the condition of without adding metal salts, only ligand H_2qldc in 8 mL H_2O was placed in a Teflon-lined stainless steel vessel (20 mL) under autogenous pressure and heated at 120 °C for 5 days. We found that the decarboxylation of free H_2qldc was performed under solvothermal conditions at 120 °C (without any other substance). The ^{13}C NMR spectra of the reaction product as well as H_2qldc are shown in Fig. S1 and Fig. S2 in the Supporting Information, in which the characteristic peaks of –*C*OOH appeared at 167.99 and 166.22 ppm, but for the reaction product only one characteristic peak of –*C*OOH appeared at 166.30 ppm. As aforementioned reaction fact, coordination polymer **Ag1** can be obtained at 80°C. Based on these facts, we can deduce that, the coordination between the ligand and the metal center may be occurred before the decarboxylation of H_2qldc in **Ag1**. Meanwhile, when **Ag1** assembling, the decarboxylation is too difficult to perform. As shown in TG curve, until 452.2 °C, **Ag1** begins to lose the two carboxylates. Compared with **Ag1**, coordination polymer **Ag2** was not obtained at 80°C (other conditions remain unchanged except for the reaction temperature). The phenomenon can be explained as: in **Ag2**, the coordination reaction may be occurred after the decarboxylation process. The aryl group in H_2qldc ligand as electron attracting group is beneficial to the cleavage of C–C bond. The reaction mechanism of **Ag1** and **Ag2** are shown in Scheme 1.

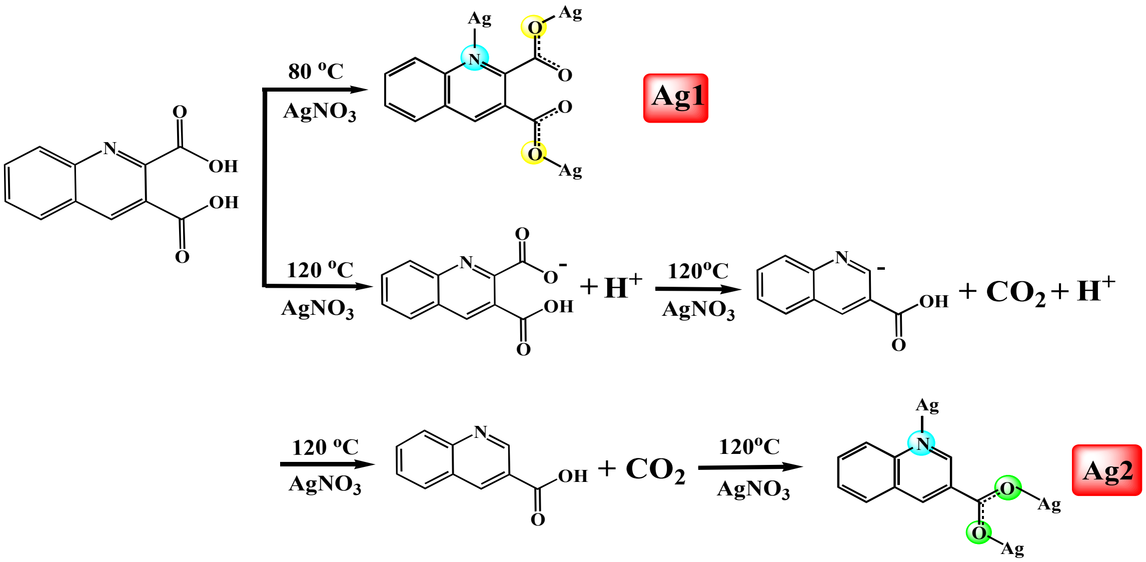

Scheme 1 The reaction mechanism of coordination polymers **Ag1** and **Ag2**.

X-Ray crystal structure determination

The X-ray diffraction data taken at room temperature for coordination polymers

Ag1 and **Cu1** are collected on a Rigaku R-AXIS RAPID IP diffractometer equipped with graphite-monochromated Mo K*α* radiation (λ = 0. 71073 Å). The structures of **Ag1** and **Cu1** are solved by direct methods and refined on F^2 by the full-matrix least squares using the SHELXTL-97 crystallographic software[18]. Anisotropic thermal parameters are refined to all of the non-hydrogen atoms. The hydrogen atoms are held in calculated positions on carbon atoms and nitrogen atoms and that are directly included in the molecular formula on water molecules. The CCDC 1036463 and 1036466 contain the crystallographic data **Ag1** and **Cu1** of this paper. These data can be obtained free of charge at www.ccdc.cam.ac.uk/ deposit. Crystal structure data and details of the data collection and the structure refinement are listed as Table 1. Selected bond lengths and bond angles for complexes are summarized in Table 2.

Table 1 Crystal data and structure refinement parameters of coordination polymers **Ag1** and **Cu1**.

Identification code	Ag1	Cu1
Empirical formula	$C_{11}H_6AgNO_4$	$C_{10}H_7CuINO_2$
Formula mass	324.04	363.61
Crystal system	Triclinic	Monoclinic
Space group	*p*-1	*P*2(1)/n
a (Å)	6.6702(13)	4.2490(8)
b (Å)	8.7729(18)	15.96232)
c (Å)	9.1647(18)	15.297(3)
α (°)	78.49(3)	90.00
β (°)	72.67(3)	90.03(3)
γ (°)	68.92(3)	90.00
V ($Å^3$)	475.13(2)	1037.5(4)
Z	2	4
D_c/(g cm^{-3})	2.265	2.328
μ (Mo Kα)/mm^{-1}	2.121	5.056
F(000)	316	688
Crystal size	0.20x 0.18 x 0.15 mm	0.14 x 0.14 x 0.12 mm
2θ range (°)	3.24 – 27.48	3.69 – 27.46
Limiting indices	$-8 \leq h \leq 8$	$-5 \leq h \leq 5$
	$-11 \leq k \leq 11$	$-20 \leq k \leq 20$
	$-11 \leq l \leq 11$	$-19 \leq l \leq 19$
Data/Restraints/Parameters	2168 / 0 / 155	2368 /0 / 136
GOF on F^2	0.983	1.267
Final *R* indices [$I > 2\sigma(I)$]		
R_1[a]	0.0324	0.0814
wR_2[b]	0.0937	0.2183
R indices (alldata)		
R_1	0.0404	0.0842
wR_2	0.0995	0.2192
CCDC	1036463	1036466

[a] $R_1 = \Sigma||F_o| - |F_c||/ \Sigma|F_o$; [b] $wR_2 = [\Sigma[w(F_o^2 - F_c^2)^2] / \Sigma[w(F_o^2)^2]]^{1/2}$.

Table 2 Selected bond lengths (Å) and bond angles (°) for coordination polymers **Ag1** and **Cu1**.

Ag1			
Ag(1)-N(1)	2.261(3)	N(1)-Ag(1)-O(1)#2	128.8(1)
Ag(1)-O(4)#3	2.390(2)	O(1)#2-Ag(1)-O(4)#3	105.4(1)
Ag(1)-O(1)#2	2.295(3)	N(1)-Ag(1)-O(4)#3	120.8(0)
Cu1			
I(1)-Cu(1)	2.645(2)	Cu(1)-I(1)-Cu(1)#1	80.4(1)
I(1)-Cu(1)#1	2.688(2)	Cu(1)-I(1)-Cu(1)#2	61.3(3)
I(1)-Cu(1)#2	2.694(3)	Cu(1)#1-I(1)-Cu(1)#2	104.3(1)
Cu(1)-N(1)	2.051(1)	N(1)-Cu(1)-I(1)	122.3(4)
Cu(1)-I(1)#1	2.688(2)	N(1)-Cu(1)-I(1)#1	109.8(4)
Cu(1)-I(1)#2	2.694(3)	I(1)-Cu(1)-I(1)#1	99.6(1)
Cu(1)-Cu(1)#2	2.723(4)	N(1)-Cu(1)-I(1)#2	100.9(4)
		I(1)-Cu(1)-I(1)#2	118.7(2)
		I(1)#1-Cu(1)-I(1)#2	104.3(1)
		N(1)-Cu(1)-Cu(1)#2	134.9(4)
		I(1)-Cu(1)-Cu(1)#2	60.2(3)
		I(1)#1-Cu(1)-Cu(1)#2	114.0(4)
		I(1)#2-Cu(1)-Cu(1)#2	58.5(5)

Symmetry transformations used to generate equivalent atoms: #1: –x, –y+2, –z; #2: –x, –y+1, –z+1.

Results and discussion

IR spectroscopy

The IR spectra of coordination polymers **Ag1**, **Ag2**, **Cu1** and the free ligand 2,3-H_2qldc are shown in Fig. S3. The asymmetric stretching vibrations of the carboxyl group in **Ag1** and **Ag2** are observed at ca. 1590 cm^{-1} and the band of symmetric stretching vibrations are observed at ca. 1394 cm^{-1}. The frequent separation between the asymmetric and symmetric stretching of carboxyl group can be mode to distinction between these binding states. The deviation $\Delta(\nu_{as}(COO^{-})–\nu_{s}(COO^{-}))$ was approximately 200 cm^{-1}, in the range of 100 cm^{-1} to 200 cm^{-1}, which indicates that the coordination interaction exists between the metal ion and the oxygen atoms of carboxyl group. Therefore, the stretching vibrations of the carboxyl group shift toward lower frequencies and the intensity is greatly reduced compared to that of free ligand (1700 cm^{-1}). The absence of strong bands ranging from 1579 to 1590 cm^{-1} for coordination polymers **Ag1** and **Ag2** indicate that the ligand in these coordination polymers are deprotonated, compared with those of free ligands in these complexes. Coordination polymer **Cu1** possesses identical ligand 2,3-H_2qldc and their IR spectra are similar. The asymmetric stretching vibration of the carboxyl group is observed at ca. 1700 cm^{-1}, and the band of symmetric stretching vibration is observed at ca. 1285 cm^{-1}, as the same as ligand 2,3-H_2qldc, which indicates that the oxygen atoms of carboxyl group does not coordinate to the metal ion. Weak bands in the region of 476–597 cm^{-1} are observed in the spectra of coordination polymers, which are assigned to ν(M–N) and ν(M–O) stretching vibrations[19]. These are in agreement with the results of single-crystal X-ray diffraction analysis.

Description of crystal structure

Crystal structure of [Ag(2,3-Hqldc)]$_n$(Ag1)

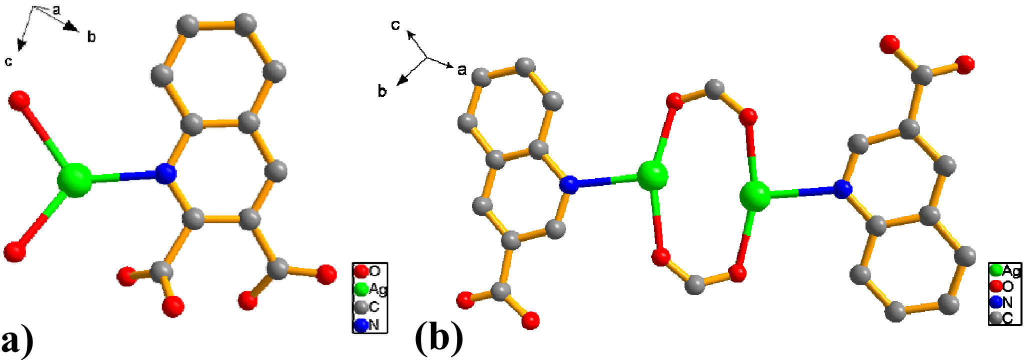

Fig. 1 The structural unit of **Ag1** (a) and **Ag2** (b) with labeling scheme and 50% thermal ellipsoids (hydrogen atoms are omitted for clarity).

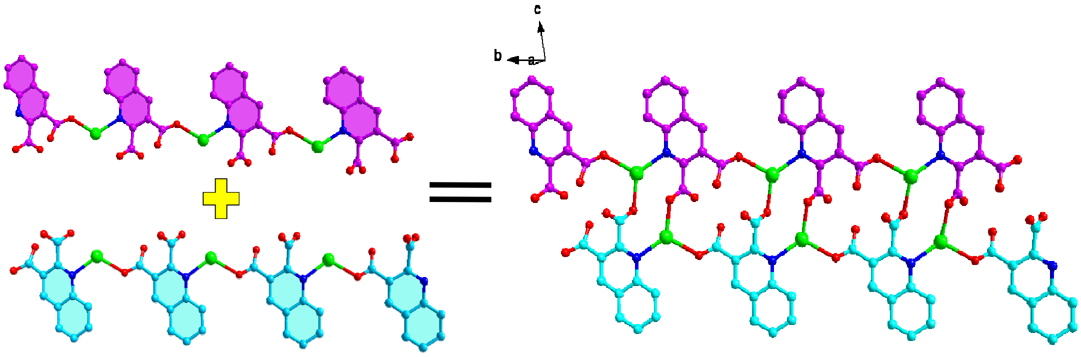

Fig. 2 Ball-and-stick representation of the 1D chain structure and the 1D+1D→1D chain structure in **Ag1**.

The 1D mononuclear coordination polymer **Ag1** crystallizes in the triclinic space group *P*-1. The asymmetric unit of **Ag1** and **Ag2** are shown in Fig. 1. The asymmetric unit of **Ag1** contains one Ag(I) cation, one 2,3-Hqldc$^-$ anion. Ag(I) center is three-coordinated by one nitrogen atom (N1) from one 2,3-Hqldc$^-$ anion and two oxygen atoms (O1A and O4A) from two other 2,3-Hqldc$^-$ anions, forming a plane triangle. Ag–N bond length is 2.261(3) Å, Ag–O bond lengths are 2.295(3) and 2.390(2) Å respectively. All Ag–N and Ag–O bond lengths as well as the bond angles around Ag(I) ion are in the range expected for such coordination polymers[1b]. Two adjacent silver ions are connected through N1 and O4 atoms deriving from one 2,3-Hqldc$^-$ anion, giving rise to an infinite 1D zigzag chain. What's more, two adjacent 1D zigzag chains are linked by bridging O atom, forming a new 1D+1D→1D chain with a Ag···Ag separation of 4.168 Å (Fig. 2). It is noteworthy that, in the **Ag1** crystal structure, it exits weak intermolecular forces including aromatic rings. Further analysis of the crystal packing reveals that adjacent 1D chains are further connected by face–to–face π···π interactions between quinoline ring with a centroid to centroid distance of 3.697 Å (Fig. 3a) and 3.785 Å (Fig. 3b). They play an important role in stabilizing the network structure, and further resulting in a 3D supramolecular architecture.

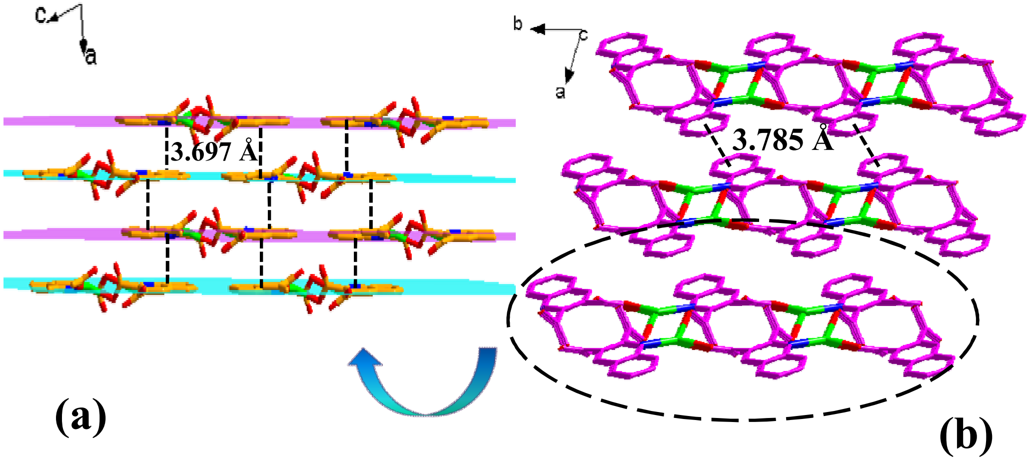

Fig. 3 (a) Stick representation of the 2D layer through π···π packing in **Ag1**; (b) Stick representation of the 3D framework structure through π···π packing in **Ag1** and all the hydrogen atoms are omitted for clarity.

Notably, though the chemical environments of the central Ag cations are the same in **Ag1** and **Ag2**, the major difference is the dihedral angle between the carboxyl and quinoline in one bridging organic ligand. The dihedral angle between the two planes in one bridging ligand is 3.70° in the **Ag2**, which is much smaller than those of 61.98° and 30.49° in **Ag1**. Hence, **Ag2** overcomes the shortcoming of the coplanarity, which is constructed by carboxyl and quinoline ring and shows fantastic coplanar structure.

Crystal structure of [CuI(3-Hqlc)]$_n$(Cu1)

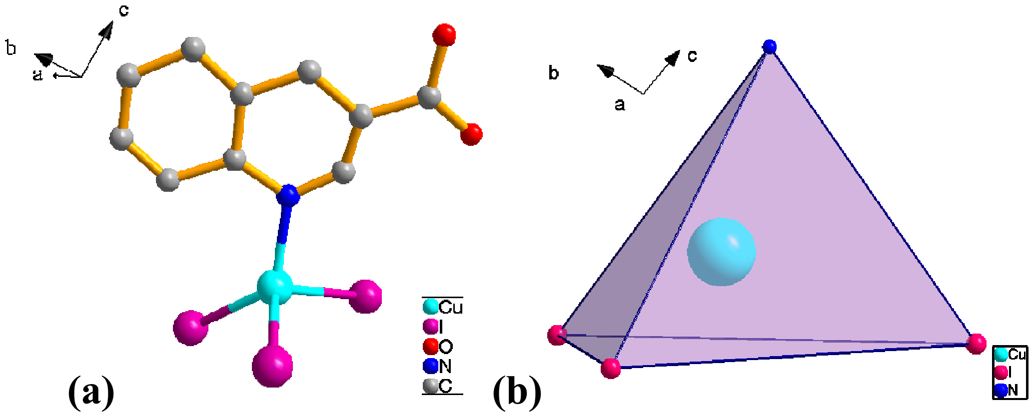

Fig. 4 (a) The structural unit of **Cu1** with labeling scheme and 50% thermal ellipsoids (hydrogen atoms are omitted for clarity). (b) Polyhedral representation of the coordination sphere of the Cu$^+$ centre, with display distorted tetrahedron arrangement in the coordination polymer **Cu1**.

Coordination polymer **Cu1** crystallizes in a monoclinic space group *P*2(1)/n and displays a 1D ladder chain structure, which further forms 2D structure by hydrogen bonding interaction. The asymmetric unit of coordination polymer **Cu1** contains one Cu(I) ion, one iodine ion and one 3-Hqlc ligand (Fig. 4). Cu(1) is coordinated by three I ions and one N atom from 3-Hqlc with Cu–N distances of 2.051(1) Å. The bridging iodine anions are coordinated simultaneously to three Cu(I) metal centers (μ_3-bridges) with slightly different coordination bond lengths span a range from 2.645(2) to 2.694(3) Å[20], which shows a rare ladder-like chain constructed by I and Cu atoms. The dihedral angle between two Cu-I planes is 66.52°. On the other hand, the 3-Hqlc ligand uses only one nitrogen atom of each quinoline ring to bridge two metal centers belonging to adjacent $[Cu_2I_2]_n$ substructures, with a Cu···Cu distance of 2.723(4) Å, which is close to the sum of the van der Waals radii of Cu atoms (2.8 Å), implying the existence of weak Cu···Cu interactions[21]. This conformation is stabilized by intermolecular hydrogen bonding. In coordination polymer **Cu1**, donor···acceptor distance in O–H···O can be found, which is ranging from 1.682 to 2.562 Å. The shortest distance 1.782 Å refers to the intermolecular O2–H2···O1 (∠OHO = 172.99°) hydrogen bond. A two-dimensional supramolecular network is formed by O-H···O hydrogen bonded interactions (Fig.5).

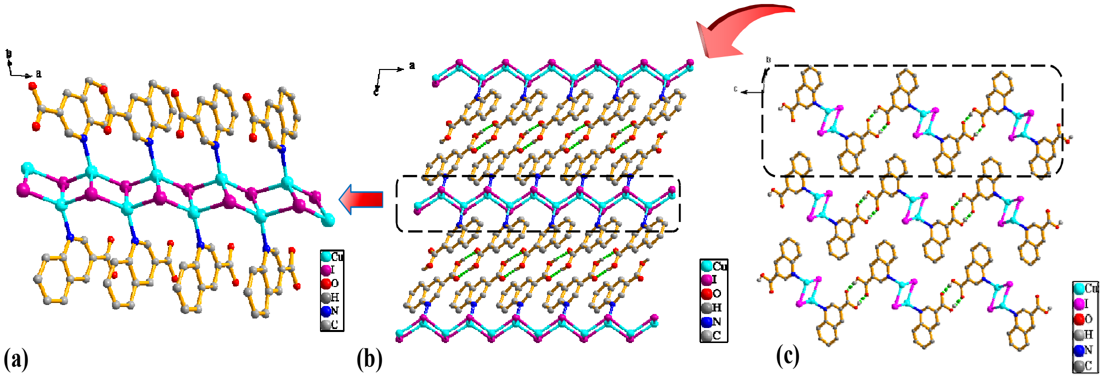

Fig. 5 Drawings of the $[Cu_2I_2]_n$ infinite chain subunit, the sheet, and the crystal packing of coordination polymer **Cu1**.

Photoluminescent properties and lifetimes of coordination polymers

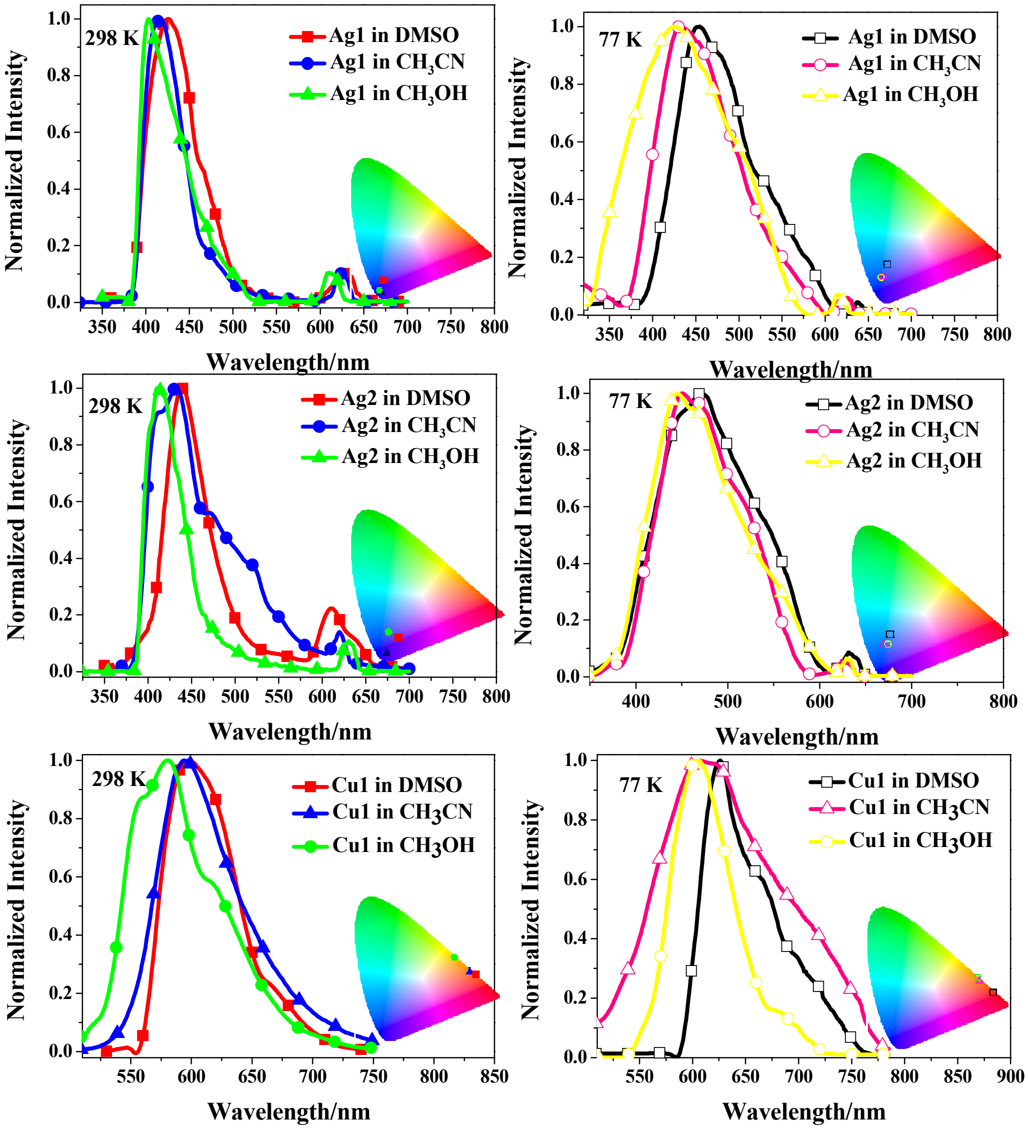

Fig. 6 Normalized emission spectra of coordination polymers **Ag1**, **Ag2** and **Cu1** in DMSO, CH_3CN and CH_3OH solutions (concentration: (M) ≈ 10^{-5} M) at 298 K and 77 K and the corresponding color coordinate diagram of emission.

Table 3 Luminescence data for coordination polymers **Ag1**, **Ag2**, **Cu1** and ligand H_2qldc.

Coordination polymers/ligands	Absorption(nm) (ε/dm^{3}cm^{-1}mol^{-1})	Excitation (λ, nm)	Emission (λ_{max}, nm)	CIE (x, y)	Quantum yields(Φ)[b]	Lifetimes (μs)					Conditions[a]
						τ_1 (μs)	A_1%	τ_2 (μs)	A_2%	<τ> (μs)	
Ag1	267 (79236)	300	427,631	0.17, 0.12	0.185	1.72	46.39	13.71	53.61	12.54	DMSO, 298K
	227 (139893)	300	416,624	0.16, 0.05	0.143	1.77	45.68	13.49	54.32	12.33	CH_3CN, 298K
	222 (84282)	300	404,611	0.15, 0.06	0.092	0.91	6.37	7.29	55.40	7.20	CH_3OH, 298K
	—	300	455	0.23, 0.29	—	0.89	54.51	7.08	45.49	6.27	Solid, 298K
	—	300	453,639	0.18, 0.22	—	1.37	51.73	18.03	48.27	16.78	DMSO, 77K
	—	300	434,626	0.16, 0.16	—	2.04	43.31	15.55	56.69	14.32	CH_3CN, 77K
	—	300	425,614	0.15, 0.15	—	1.12	40.59	13.02	59.41	12.36	CH_3OH, 77K
	—	300	476	0.23, 0.30	—	1.81	54.10	18.10	45.90	16.38	Solid, 77K
Ag2	276 (63000)	300	446,609	0.23, 0.14	0.254	1.16	49.43	11.29	50.57	10.37	DMSO, 298K
	222 (54294)	300	431,618	0.17, 0.06	0.212	1.44	64.73	10.99	35.27	9.14	CH_3CN, 298K
	215 (91294)	300	412,628	0.18, 0.17	0.126	1.12	56.03	10.03	43.97	8.92	CH_3OH, 298K
	—	300	446	0.23, 0.27	—	1.20	50.40	8.33	49.60	7.42	Solid, 298K
	—	300	471,632	0.18, 0.26	—	1.29	48.60	13.03	51.40	12.03	DMSO, 77K
	—	300	452,628	0.15, 0.21	—	1.09	57.14	12.37	42.86	11.18	CH_3CN, 77K
	—	300	445,631	0.17, 0.21	—	1.25	56.00	10.89	44.00	9.66	CH_3OH, 77K
	—	300	479	0.24, 0.33	—	1.74	43.02	19.02	56.98	17.90	Solid, 77K
Cu1	297 (75669)	360	602	0.61, 0.39	0.283	1.40	50.24	16.07	49.76	14.88	DMSO, 298K
	276 (97888)	360	590	0.58, 0.41	0.224	1.71	47.03	13.17	52.97	11.99	CH_3CN, 298K
	274 (76551)	360	578	0.50, 0.49	0.151	1.09	44.33	11.47	55.67	10.74	CH_3OH, 298K
	—	360	576	0.51, 0.48	—	1.98	40.38	14.85	59.62	13.78	Solid, 298K
	—	360	627	0.65, 0.34	—	1.84	52.33	28.11	47.67	26.35	DMSO, 77K
	—	360	612	0.57, 0.43	—	1.22	46.15	17.14	53.85	16.22	CH_3CN, 77K
	—	360	606	0.57, 0.43	—	1.12	51.29	13.00	48.71	12.01	CH_3OH, 77K
	—	360	646	0.67, 0.30	—	2.58	46.03	22.50	53.97	1.847	Solid, 77K
H_2qldc	274 (24939)	300	434	0.20, 0.20	0.016	—	—	—	—	—	DMSO, 298K
	237 (71200)	300	419	0.16, 0.06	0.012	—	—	—	—	—	CH_3CN, 298K
	235 (101444)	300	406	0.18, 0.12	0.008	—	—	—	—	—	CH_3OH, 298K
	—	300	398	0.20, 0.19	—	—	—	—	—	—	Solid, 298K

a Concentration in DMSO, CH_3CN and CH_3OH solutions: (M) = 1×10^{-5} M.

b Determined using quinine sulfate in 0.1 M sulfuric acid (Φ = 0.546) for **Ag1**, **Ag2** and Rhodamine B chloride in ethanol (Φ = 0.690) for **Cu1** as a standard

The emission spectra of **Ag1**, **Ag2** and **Cu1** are recorded in different solvents and in the solid state at 298 K and 77 K. The photoluminescent data for emission are gathered in Table 3. To investigate the details of surrounding environment effects, the emission spectra of **Ag1**, **Ag2** and **Cu1** in solutions (DMSO, CH_3CN and CH_3OH) with the same concentration (1.0×10^{-5} mol L^{-1}) were examined by luminescence spectrophotometry at 298 K and 77 K. The ^1H NMR data indicates that **Ag1**, **Ag2** and **Cu1** still keep polymeric structure in solutions and don't decompose (Fig. S6, S7 and S8). As shown in Fig. 6, there are high energy (HE) emission and low energy (LE) emission in **Ag1** and **Ag2**. The corresponding maximum emissions are observed at 427 and 631 nm in DMSO (416 and 624 nm in CH_3CN, 404 and 611 nm in CH_3OH) for **Ag1**, and 446 and 609 nm in DMSO (431 and 618 nm in CH_3CN, 412 and 628 nm in CH_3OH) for **Ag2**. The luminescence spectra of **Ag1** and **Ag2** show that the HE peaks probably result from intraligand transitions in H_2qldc, and the Ag atoms may play some role in these transitions[22]. What's more, the LE emissions should be, without doubt, phosphorescence because of their long wavelengths and long lifetime in microsecond scale[23]. In addition, the maximum emission band for coordination polymer **Cu1** is located at 602 nm in DMSO (590 nm in CH_3CN, 578 nm in CH_3OH), upon excitation at 360 nm at 298 K, The red-shifted emission compared with ligand H_2qldc can be assigned to metal-to-ligand charge transfer (MLCT), a combination of iodide-to-copper charge transfer (XMCT) and d–s transitions in **Cu1**[24](Scheme 2). The change of temperature from 298 K to 77 K[25] caused the red shift of the emission peaks substantially in all the solutions of **Ag1**, **Ag2** and **Cu1**, the emission peaks show rich structural features at 77 K. Such fascinating phenomenon may be attributed to the different state of solution at the low temperature. At 77 K， the viscosity of the solvent increases, and the interaction between fluorescent substance and solvent, the forces of attraction and hydrogen bonds may be stronger in contrast with those at 298 K. In this case, excited state is more stable, and the energy level difference between ground state and excited state decreases. Accordingly, the luminescent emission peaks of **Ag1**, **Ag2** and **Cu1** in solution display red shifts significantly from 298 K to 77 K.

The luminescence quantum yields of coordination polymers **Ag1**, **Ag2**, **Cu1** and H_2qldc are determined in DMSO, CH_3CN, and CH_3OH. The value of the quantum yields for H_2qldc in DMSO, CH_3CN and CH_3OH are 0.016, 0.012 and 0.008, respectively, while those of **Ag1** are 0.185, 0.143 and 0.092 (0.254, 0.212 and 0.126

for **Ag2**, 0.283, 0.224 and 0.151 for **Cu1**). The quantum yields of **Ag1**, **Ag2** and **Cu1** are much higher than that of the free ligand, which can be easily explained by aggregation of the pure ligands in the solvents, which would also be in accordance with their low quantum yield. Complexation with the silver or copper might make aggregation and π-stacking more difficult than for the pure ligands and when coordination polymers assemble, the enhancement after the connection of the ligand to metal center increases the conformational rigidity of the ligands, and the loss of energy via thermal vibration decay may be reduced. Compared with coordination polymers **Ag1**, **Ag2** and **Cu1**, the luminescence quantum yields of **Ag2** and **Cu1** is significantly higher than **Ag1**, which is attributed to the decarboxylation effect. After decarboxylation making the dihedral angle of carboxyl and quinoline decreases and **Ag1** has two dihedral angles are 61.98° and 30.49° respectively. However, dihedral angle of **Ag2** is 3.70° and **Cu1** is 5.47°. The nice coplanar feature of the structure in **Ag2** and **Cu1** can enhance the mobility of π electrons in organic aromatic rings, which is in favor of luminescent emission.

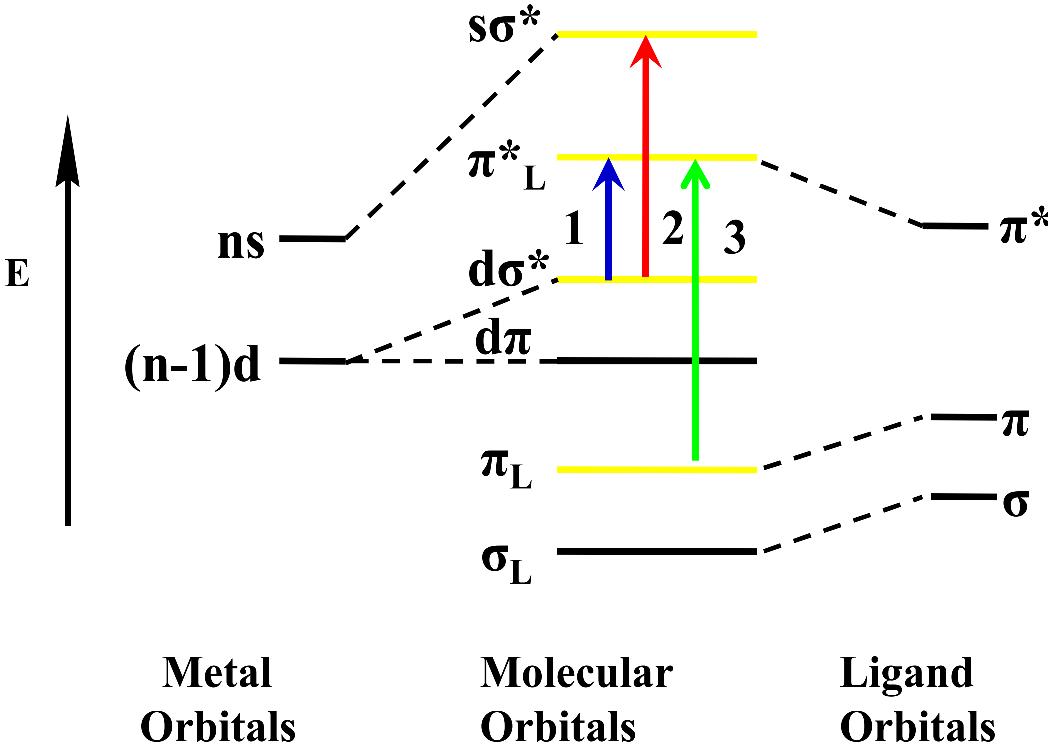

Scheme 2 Schematic energy level diagram of coordination polymers **Ag1**, **Ag2** and **Cu1** molecular orbitals (1,MLCT; 2, d–s transitions, 3, intraligand transitions).

In the solid state, the maximum emission band for coordination polymer **Ag1** is located at 455 nm (446 nm for **Ag2**), upon excitation at 300 nm, exhibiting blue emissions at 298 K. The solid-state fluorescence spectra of **Ag1** and **Ag2** exhibit strong red-shifted photoluminescence emission in comparison with that of free H_2qldc ligand (λ_{em} = 398 nm). It is noted that there is no emission band for H_2qldc ligand can be observed in the region, the photoluminescence origin of the emission bands for the coordination polymers **Ag1** and **Ag2** should be attributed to MLCT[22b, 26](Scheme 2). At 77 K, the emission band for coordination polymer **Ag1** is located at 476 nm and **Ag2** is located at 479 nm (λ_{ex} = 300 nm), exhibiting blue emissions in the solid state (Fig. 7), which shows that Ag(I) coordination polymers can be used as stable blue materials. The change of temperature from 298 K to 77 K causes a bathochromic shift of emission peaks in the solid state of **Ag1** and **Ag2**. Obviously, the red shift of coordination polymer **Ag2** is longer than **Ag1**, which due to the existence of Ag-Ag interaction in **Ag2**. Meanwhile, one of carboxyl removed, making the nice coplanar feature of the structure in **Ag2** and improve the mobility of π electrons in organic aromatic rings, so that it shows the excellent luminescence. **Ag2** shows stable luminescence at 298 K and 77 K in the solid state with the CIE color shifts from deep-blue (0.23, 0.27) to light blue (0.24, 0.33). Both **Ag1** and **Ag2** display stable blue luminescent in the solid state at 298 K and 77 K. The luminescent lifetimes for **Ag1** and **Ag2** in the solid state are determined. The luminescent lifetimes for **Ag1** at 298 K and 77 K are 6.27 μs and 16.38 μs, respectively, while those of **Ag2** are 7.42 μs and 17.90 μs. The luminescent lifetimes of **Ag1** and **Ag2** at 77 K are more than twice as those at 298 K in the solid state. A general trend is that the lifetime of emission of low-temperature (77 K) is longer than that in room temperature (298 K), which is attributed to the decrease of thermal vibration and nonradiative transition at low temperature[27].

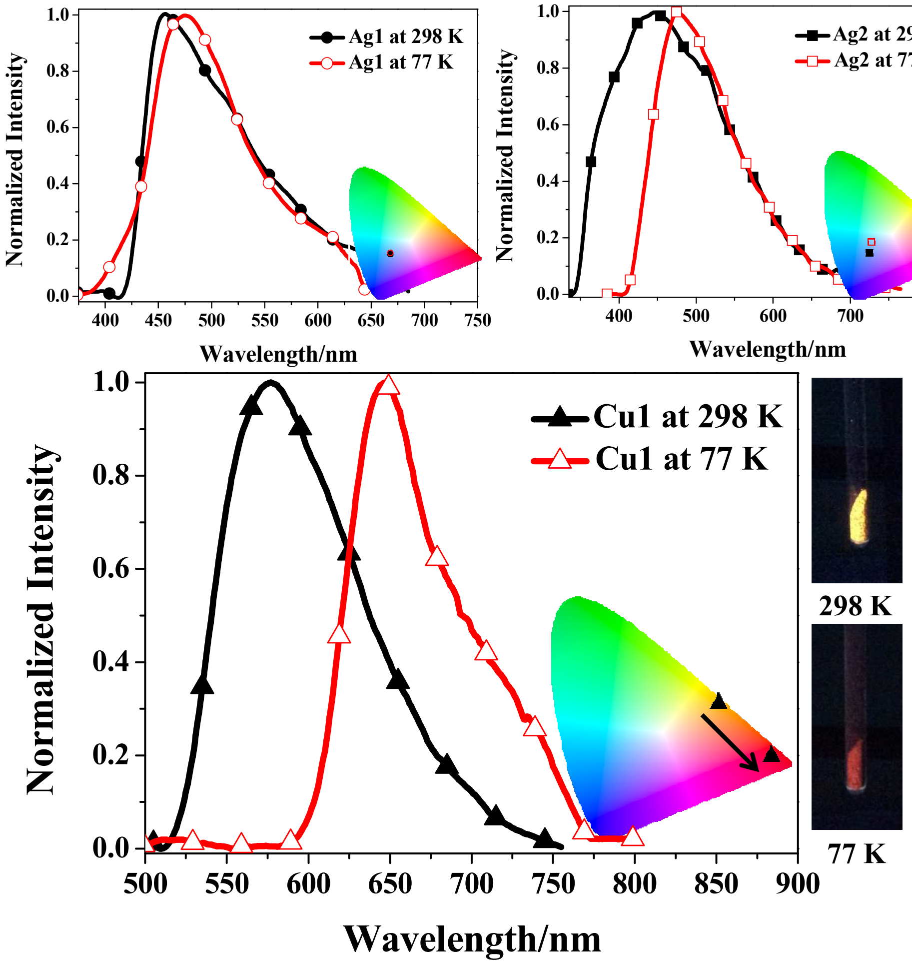

Fig. 7 Normalized emission spectra of coordination polymers **Ag1**, **Ag2 and Cu1** in the solid state at 298 K and 77 K and the corresponding color coordinate diagram of emission.

Coordination polymer **Cu1** is different from **Ag1** and **Ag2** in the solid state, under UV irradiation, at room temperature, **Cu1** emits an intense yellow light. The fascinating and visually impressive phenomenon of thermochromic luminescence of **Cu1** is revealed by immersing the samples into liquid nitrogen (77 K). When exposed to UV light, the crystalline solid shows a color changing process from bright yellow luminescence at room temperature to red luminescence at low temperature of liquid nitrogen. Once the samples gradually warmed up to room temperature, the yellow emission is recovered, indicating a reversible thermochromic luminescence for **Cu1**. The variable temperature luminescence spectrum is shown in Fig. 7. **Cu1** shows tunable luminescence at 298 K and 77 K in the solid state. The emission maximum shifts from 576 nm to 646 nm in the solid state luminescence spectrum when the temperature is decreased from 298 to 77 K. The red shift of 70 nm for **Cu1** is large enough to make the color change visible by the naked eye and the CIE color shifts from bright yellow (0.51, 0.48) to red (0.67, 0.30). Their emission bands could be attributed to triplet cluster-centered (^{3}CC) excited states, a combination of XMCT and d–s transitions[21](Scheme 2). The solid state lifetimes at room temperature is on the scale of microseconds (13.78 and 20.73 μs at 298 K and 77 K respectively), suggestive of their phosphorescent character. The long decay lifetime displayed by the Cu(I) coordination polymer, characteristic of triplet state emission.

Thermal analysis and XRPD patterns of Ag1, Ag2 and Cu1

Thermogravimetric experiments were conducted to study the thermal stability of coordination polymers **Ag1**, **Ag2** and **Cu1** (Fig. S9). The experiments were performed on samples consisting of numerous single crystals in the 25–700 °C range. The TG curve shows that **Ag1** has two weight-loss stages. The loss of 53.49% occurring at the first step is attributed to decomposition of 3-Hqlc in the range of 238.1~251.8 °C (calculated 53.44%). The second weight-loss of 13.22% at 452.2~556°C can be ascribe to loss the 2-position carboxyl (calculated 13.58%). The TG curve of **Ag2** shows the coordination polymer is very steady and there is no weight loss until 245.8 °C, the first weight-loss of 8.01% which corresponding to loss the 3-position carboxyl (calculated 7.86%) and the following weight-loss of 53.57% during 338.2~367.2°C, which is attributed to the decomposition of the 3-qlc ligands (calculated 53.62%). The remaining weight of 33.29% for **Ag1** and 38.42% for **Ag2**， corresponds to the percentage (calculated 32.98% and 38.52%) of the Ag components, indicating that the final product is metal Ag. Through analyzing the TG curves of **Ag1** and **Ag2**, we deduce that once 2-position carboxyl coordinates to Ag atom, the sample is very steady and it begins to lose the weight until 452.2 °C in **Ag1**. In the TG curve of **Cu1**, there are two weight-loss steps. The loss 45.74% occurring at the first step is attributed to the sublimation of I_2 and lose the weight of 3-position carboxyl in the range of 237.8~320.4°C (calculated 45.29%). The second weight-loss of 31.63% at 320.4~402.9°C corresponds to the decomposition of quinoline (calculated 33.76%). The remaining weight of 22.63% for **Cu1**, the observed weight loss of 22.63% is in good agreement with the calculated value (20.95%), indicating that the final product is CuO.

The XRPD patterns for coordination polymers **Ag1**, **Ag2** and **Cu1** are shown in Fig. S10. The diffraction peaks of both simulated and experimental patterns match well in key positions, indicating thus the phase purities of coordination polymers **Ag1**, **A g2** and **Cu1.**

Properties of PMMA polymer doped with coordination polymer Cu1

TG analysis of **Cu1**@PMMA film exhibits no weight-loss in the temperature range of 25–285 °C in contrast to that for coordination polymer **Cu1** (Fig. 8). Furthermore, TG analysis of **Cu1**@PMMA film shows a slight increase of 48 °C in comparison with the pure PMMA, which suggests that the thermal stability of the **Cu1**@PMMA film is essentially improved by doping coordination polymer **Cu1**. The IR spectra of **Cu1**, PMMA and **Cu1**@PMMA are shown in Fig. S11.

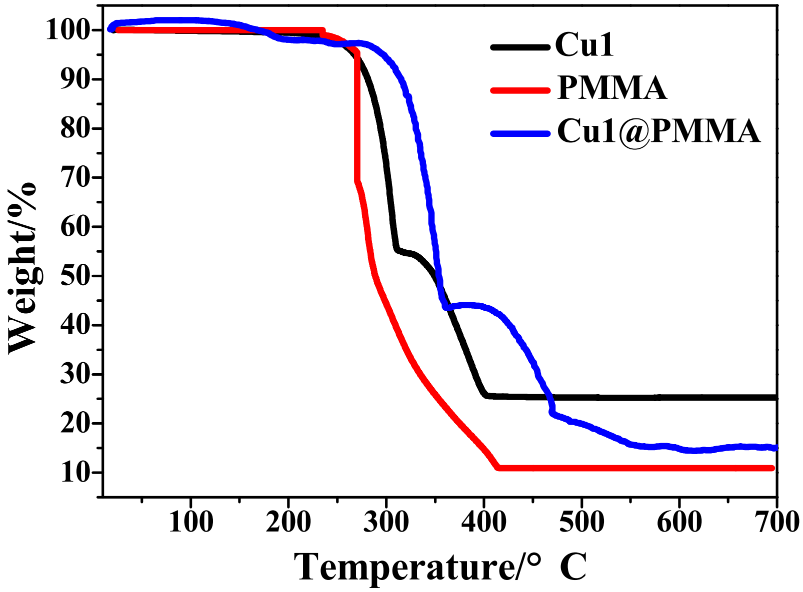

Fig. 8 The comparison TG curves of pure **Cu1**, PMMA, and **Cu1**@PMMA.

Based on the excellent luminescence of Cu(I) coordination polymers, making it incorporated into polymer matrixes represents a new class of materials. The materials can serve as ideal candidates in the pursuit of application in farm plastic–film with optical transfer function[28]. As an extension of this work, we describe the incorporation of the newly designed, and intensity luminescent **Cu1** into PMMA, a low–cost and easily prepared polymer with excellent optical quality. The excitation spectrum of the PMMA polymer films doped with **Cu1** at different concentrations [0.2, 0.4, 0.6, 0.8, 1.0, 1.2 and 1.4% (w/w)] is shown in Table 4. The emission spectrum of PMMA doped with coordination polymer **Cu1** is at 578 nm (λ_{ex} = 360 nm). The lifetimes for coordination polymer **Cu1** and the PMMA matrixes doped with coordination polymer

Cu1 are listed in Table 4. Noticeably, with the increase of the content of coordination polymer **Cu1**, the lifetime of the **Cu1**@PMMA films increases and reaches a maximum at 1.0% and then decreases with further increasing of the content of coordination polymer **Cu1** (Fig. 9). It can be attributed to the fact that with a low concentration of coordination polymer **Cu1** in the PMMA polymer, the coordination polymer **Cu1** can disperse uniformly in the PMMA matrix and the PMMA effectively sensitizes the luminescence of the coordination polymer **Cu1**. Upon further increasing of the content of coordination polymer **Cu1** to more than 1.0%, some aggregates formed in the film and the excition migration between the **Cu1** resulted in the luminescence quenching of coordination polymer **Cu1**[29]. Noticeably, with the increasing of the content of **Cu1**, the lifetime of **Cu1**@PMMA films reaches a maximum at 1.0% (τ = 95.57 μs), which is more than eight times longer than that of **Cu1** (τ = 13.78 μs). All *τ* values for the doped polymer systems are higher than coordination polymer **Cu1**, indicating that radiative processes are operative in all the doped polymer films. **Cu1**@PMMA is confirmed as a yellow luminescence polymer film material.

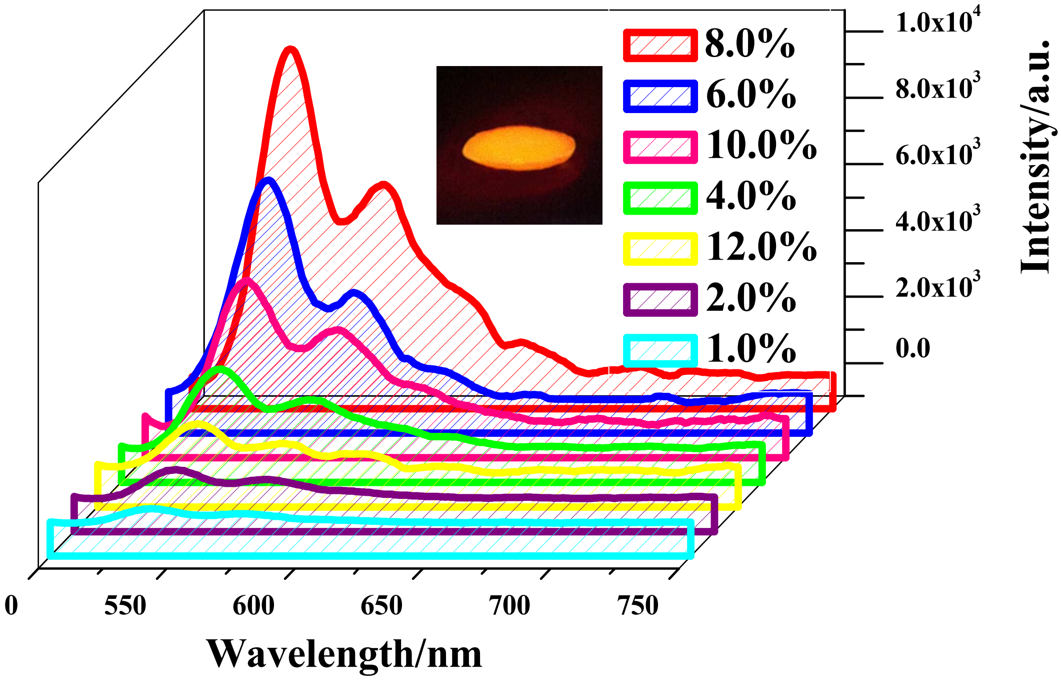

Fig. 9 The emission spectra of PMMA polymer doped with coordination polymer **Cu1** in 0.2–1.4 % at 298 K under excitation at 360 nm.

Table 4 Luminescence data for coordination polymer **Cu1** and **Cu1**@PMMA

	Excitation (λ, nm)	Emission (λ_{max}, nm)	Integrated Area	Lifetimes (μs)				
				τ_1 (μs)	A_1%	τ_2 (μs)	A_2%	<τ> (μs)
Cu1@0.2%PMMA	360	578	24862.07	1.17	8.66	35.86	91.34	37.75
Cu1@0.4%PMMA	360	578	88384.10	1.41	8.75	46.05	91.25	45.92
Cu1@0.6%PMMA	360	578	160371.01	1.18	6.44	50.26	93.56	50.18
Cu1@0.8%PMMA	360	578	229682.46	1.01	4.25	83.43	95.75	83.39
Cu1@1.0%PMMA	360	578	334392.39	2.08	2.93	95.63	97.07	95.57
Cu1@1.2%PMMA	360	578	72764.47	1.13	9.42	47.14	90.58	47.03
Cu1@1.4%PMMA	360	578	31401.74	1.03	8.57	43.69	91.43	43.60

Conclusion

In summary, three 1D coordination polymers $[Ag(2,3\text{-}Hqldc)]_n$(**Ag1**)，$[Ag(3\text{-}qlc)]_{2n}$(**Ag2**) and $[CuI(3\text{-}Hqlc)]_n$(**Cu1**) were successfully synthetized under hydro(solvo) thermal methods based on quinoline-2,3-dicarboxylic acid (H_2qldc). Through controlling the temperature makes the ligand H_2qldc decarboxylation and results in the formation of 3-Hqlc ligand. After decarboxylation, the nice coplanar feature of the structure in **Ag2** can enhance the luminescent efficiency. Both **Ag1** and **Ag2** display stable blue luminescent in the solid state and in solvents (DMSO, CH_3CN and CH_3OH) at 298 K and 77 K. The luminescent lifetimes of **Ag1** and **Ag2** at 77 K are longer than at 298 K both in the solid state and in solvents. The quantum yields of **Ag1** and **Ag2** are much higher than those of free ligand. The superior photoluminescent properties make coordination polymers **Ag1** and **Ag2** promising materials for the development of optical devices. While **Cu1** shows tunable luminescence by changing the temperature from 298 K to 77 K in the solid state, the luminescence variation from bright yellow to red indicating thermochromic luminescence for **Cu1**. In extending work, **Cu1** is doped with PMMA matrix to obtain PMMA–supported doped polymer film materials, which displays excellent yellow luminescent properties with enhanced luminescent intensities, long lifetimes and thermal stability, thus it can be used in the pursuit of application in farm plastic–film with optical transfer function.

Acknowledgements

This work was supported by the National Natural Science Foundation of China (Grant 21371040 and 21171044), the National key Basic Research Program of China (973 Program, No. 2013CB632900), and the Fundamental Research Funds for the

Central Universities (Grant No. HIT. IBRSEM. A. 201409), also Program for Innovation Research of Science in Harbin Institute of Technology (PIRS of HIT No. A201416 and B201414).

References

1 (a) Y. Y. Tang, C. X. Ding, S. W. Ng and Y. S. Xie, *RSC Advances*, 2013, 3, 18134; (b) B. Li, R. W. Huang, H. C. Yao, S. Q. Zang and T. C. W. Mak, *CrystEngComm.*, 2014, 16, 723.

2 I. Takashima, A. Kanegae, M. Sugimoto and A. Ojida, *Inorg. Chem.*, 2014, 53, 7080.

3 S. Y. Liu, X. L. Qi, R. B. Lin, X. N. Cheng, P. Q. Liao, J. P. Zhang and X. M. Chen, *Adv. Funct. Mater.*, 2014, 24, 5866.

4 K. Kuriki and Y. Koike, *Chem. Rev.*, 2002, 102, 2347.

5 L. Shi, Z. Liu, G. Dong, L. Duan, Y. Qiu, J. Jia, W. Guo, D. Zhao, D. Cui and X. Tao, *Chem. Eur. J.*, 2012, 18, 8092.

6 Q. Zhu, C. Shen, C. Tan, T. Sheng, S. Hu and X. Wu, *Chem. Commun.*, 2012, 48, 531.

7 (a) S. Q. Liu, H. Konaka, Y. Suenaga, M. Maekawa,T. Mizutani, G. L. Ning and M. Munakata, *Inorg. Chem.*, 2005, 44, 1031; (b) Y. B. Dong, J. P. Ma and R. Q. Huang, *Inorg. Chem.*, 2006, 45, 3325.

8 W. Q. Fan, J. Feng, S. Y. Song, Y. Q. Lei, G. L. Zheng and H. J. Zhang, *Chem. Eur. J.*, 2010, 16, 1903.

9 (a) W. Li, P. Yan, G. Hou, H. Li and G. Li, *Dalton Trans.*, 2013, 42, 11537; (b) H. G. Liu, S. Park, K. Jang, X. S. Feng, C. Kim, H. J. Seo and Y. I. Lee, *J. Lumin.*, 2004, 106, 47.

10 D. G. Cuttell, P. E. Fanwick, D. R. McMillin and R. A. Walton, *J. Am. Chem. Soc.*, 2002, 124, 6.

11 W. L. Jia, Y. Tao, J. P. Lu and S. N. Wang, *Inorg. Chem.*, 2005, 44, 5706.

12 (a) Z. M. Hudson, C. Sun, M. G. Helander, Y. L. Chang, Z. H. Lu and S. Wang, *J. Am. Chem. Soc.*, 2012, 134, 13930; (b) P. Myllymaki, M. Roeckerath, J. M. Lopes, J. Schubert, K. Mizohata, M. Putkonen and L. Niinisto, *J. Mater. Chem.*, 2010, 20, 4207.

13 (a) M. F. Wang, X. J. Hong, Q. G. Zhan, H. G. Jin, Y. T. Liu, Z. P. Zheng, S. H. Xu and Y. P. Cai, *Dalton Trans.*, 2012, 41, 11898; (b) X. J. Hong, M. F. Wang, H. Y. Jia, W. X. Li, J. Li, Y. T. Liu, H. G. Jin and Y. P. Cai, *New J. Chem.*, 2013, 37, 933.

14 Y. Gong, M. M. Zhang, J. B. Qin, J. Li, J. P. Meng and J. H. Lin, *Dalton Trans.*, 2014, 43, 8454.

15 C. B. Liu, Q. Li, X. Wang, G. B. Che and X. J. Zhang, *Inorg. Chem. Commun.*, 2014, 39, 56.

16 C. B. Liu, Y. Cong and H. Y. Sun, *Acta crystallographica. Section E, Structure reports online*, 2012, 68, m1177.

17 L. Li, J. Luo, S. Wang, Z. Sun, T. Chen and M. Hong, *Cryst. Growth Des.*, 2011, 11, 3744.

18 (a) G. M. Sheldrick, 1997; (b) G. M. Sheldrick, 1997.

19 G. C. Xu, L. Zhang, Y. H. Zhang, J. X. Guo, M. Q. Shi and D. Z. Jia, *CrystEngComm.*, 2013,

15, 2873.

20 B. Liu, S. F. Pan and W. Z. Chen, *Inorg. Chem.*, 2014, 53, 10485.

21 D. Sun, S. Yuan, H. Wang, H. F. Lu, S. Y. Feng and D. F. Sun, *Chem. Commun.*, 2013, 49, 6152.

22 (a) J. Zheng, Y. D. Yu, F. F. Liu, B. Y. Liu, G. Wei and X. C. Huang, *Chem. Commun.*, 2014, 50, 9000; (b) K. K. Bisht, A. C. Kathalikkattil and E. Suresh, *RSC Advances*, 2012, 2, 8421.

23 J. P. Zhang, X. C. Huang and X. M. Chen, *J. Am. Chem. Soc.*, 2005, 127, 5495.

24 (a) D. Braga, L. Maini, P. P. Mazzeo and B. Ventura, *Chem. Eur. J.*, 2010, 16, 1553; (b) J. Song, Y. Hou, L. Zhang and Y. Fu, *CrystEngComm.*, 2011, 13, 3750; (c) Z. L. Fang, X. Y. Wu, R. M. Yu and C. Z. Lu, *CrystEngComm.*, 2014, 16, 8769.

25 (a) E. C. Constable, M. Neuburger, P. Rosel, G. E. Schneider, J. A. Zampese, C. E. Housecroft, F. Monti, N. Armaroli, R. D. Costa and E. Orti, *Inorg. Chem.*, 2013, 52, 885; (b) P. Ivanov, S. Stanimirov, S. Kaloyanova and I. Petkov, *J. Fluoresc.*, 2012, 22, 1501.

26 Y. Y. Liu, Y. Y. Xu, Y. Y. Wang, J. Z. Huo, B. Ding, Y. Wang and X. G. Wang, *Z. Anorg. Allg. Chem.*, 2014, 640, 2463.

27 A.V. Dijken, D. Vanmaekelbergh, A. Meijerink , *J. Phys. Chem. B*, 2000, 104, 1715.

28 D. B. Raj, B. Francis, M. L. Reddy, R. R. Butorac, V. M. Lynch and A. H. Cowley, *Inorg. Chem.*, 2010, 49, 9055.

29 W. Li, P. Yan, G. Hou, H. Li and G. Li, *RSC Advances*, 2013, 3, 18173.